Available online at www.sciencedirect.com
ScienceDirect
Catalysis Today 131 (2008) 464–471
CATALYSIS TODAY
www.elsevier.com/locate/cattod

The hydrocracking of *n*-decane over bifunctional Ni-$H_3PW_{12}O_{40}/SiO_2$ catalysts

Bo Qiu, Xiaodong Yi *, Ling Lin, Weiping Fang *, Huilin Wan

State Key Laboratory for Physical Chemistry of the Solid Surfaces, College of Chemistry and Chemical Engineering, Xiamen University, Xiamen 361005, PR China

Available online 7 January 2008

Abstract

A series of bifunctional Ni-$H_3PW_{12}O_{40}/SiO_2$ catalysts for the hydrocracking of *n*-decane were designed and prepared. The evaluation results of the catalysts show that Ni-$H_3PW_{12}O_{40}/SiO_2$ catalysts possess a high activity for hydrocracking of *n*-decane and an excellent tolerance to the sulfur and nitrogen compounds in the feedstock. Under the reaction conditions: reaction temperature 300 °C; H_2/*n*-decane volume ratio of 1500; total pressure of 2 Mpa and the LHSV 2 h^{-1}, the conversion of *n*-decane over reduced 5%Ni-50%$H_3PW_{12}O_{40}/SiO_2$ catalysts is as high as 90%, the C_5^+ selectivity equal to 70%. In order to reveal the structure and nature of the catalysts, a number of characterizations including XRD, Raman, H_2-TPD, NH_3-TPD, XPS and FT-IR of pyridine adsorption were carried out. The characteristic results show that the high activity of the catalysts and high C_5^+ selectivity can be related to the unique structure of the $H_3PW_{12}O_{40}$ and its suitable acidity.

Keywords: Hydrocracking; Bifunctional catalyst; Ni; $H_3PW_{12}O_{40}$; Decane

1. Introduction

High-pressure hydrocracking is a catalytic refining process allowing the conversion of rather heavy petroleum fractions such as vacuum distillates into gasoline or middle distillates [1,2]. The hydrocracking process attracts more and more interests because of its great versatility and the function to equilibrate the supply and demand of light fractions [1,3]. In order to minimize the environmental impact of automotive fuels, the need of high-quality diesel fuels is found to be increasing. Obviously, the hydrocracking which ensures the elimination of sulfur and nitrogen-containing compounds as well as a deep saturation of aromatics will be more and more important in the near future [1,4].

In the 1950s, the bifunctional catalysts consisting of both highly dispersed metals for hydrogenation or dehydrogenation and an acidic support for cracking or isomerization were introduced in refining processes such as hydrocracking [5]. Conventionally, a suitable transition metal (Pt, Pd, Ni and Co) has been applied as the main active metal component, which is deposited on the acidic supports. The noble metals over some supports demonstrate excellent promoting effects in both the activity and stability of the catalysts for the hydrocracking and hydroconversion. However, they display a low resistance to sulfur poisoning [2,3]. In comparison with high cost of noble metals, metal Ni is usually chosen to be replacement of noble metals in some reactions for its good reducibility and low cost. Metals supported on zeolites have received much attention for their use as hydrocracking and hydroisomerization catalysts [6]. The strong acidity of zeolites will favor successive cracking reactions of the feed molecules, leading to the formation of the desired light products [7]. However, it also increases both the amount of coke deposition caused by polymerization of feedstock and undesirable cracking products generated by excess cracking and it is easily to be poisoned by nitrogen-containing compounds or polycyclic aromatic compounds [7,8]. Furthermore, due to the limitation of the pore size, the large feed molecules are restricted to approach the active sites. Hence, much effort has been devoted to find a good support with larger pore size and suitable acidity.

$H_3PW_{12}O_{40}$ is a polyoxotungstate [9] made up of heteropoly anions having a basic structural unit of metal–oxygen octahedra. The heteropoly acids, environmentally friendly

* Corresponding authors. Tel.: +86 592 2186291; fax: +86 592 2183047.
E-mail addresses: xdyi@xmu.edu.cn (X. Yi), wpfang@xmu.edu.cn (W. Fang).

0920-5861/$ – see front matter © 2007 Published by Elsevier B.V.
doi:10.1016/j.cattod.2007.10.095

solid acids catalysts, which offer several advantages in terms of catalytic performance, strong acid and redox sites [9], have been used in some reactions. However, there is little report about its activity for hydrocracking. Thus, it is of great interest to develop new hydrocracking catalysts composed of $H_3PW_{12}O_{40}$ [10] as acid sites and Ni as the metal sites [1,5].

In the present paper, a series of Ni-$H_3PW_{12}O_{40}/SiO_2$ catalysts were prepared by impregnation method and characterized by XRD, Raman, H_2-TPD, NH_3-TPD, XPS and FT-IR of pyridine adsorption. The evaluation results show that Ni-$H_3PW_{12}O_{40}/SiO_2$ catalysts possess a high activity for the hydrocracking of *n*-decane and display an excellent tolerance to the sulfur and nitrogen compounds in the feedstock. The catalytic activity was discussed in relation to the structure and the surface acid properties of the catalysts.

2. Experimental

2.1. Catalyst preparation

The Ni/SiO_2 catalysts were prepared by impregnation of silica support (commercial product, specific surface area 406 $m^2\ g^{-1}$) with a solution containing the desired quantities of $Ni(NO_3)_2$. Impregnated samples were dried overnight at 120 °C and then calcined in air at 400 °C for 3 h.

The Ni-$H_3PW_{12}O_{40}/SiO_2$ catalysts were prepared by impregnation of Ni/SiO_2 catalysts with a solution containing the desired quantities of $H_3PW_{12}O_{40}$. After impregnation, samples were dried overnight at 120 °C without calcine. But, it will be calcined in air at different temperature whenever it is needed.

Samples prepared with different amount of nickel (5%, 10% and 15%) and different amount of $H_3PW_{12}O_{40}$ were labeled as *x*Ni-*y*HPW/SiO_2, wherein "*x*" and "*y*" stand for wt% content of Ni and $H_3PW_{12}O_{40}$ in the catalysts respectively, while the HPW stands for the $H_3PW_{12}O_{40}$.

2.2. Catalyst characterization

The surface area (BET) and pore volume of the catalysts were determined by means of nitrogen adsorption at −194 °C on an adsorption automatic instrument (Micromeritics Tristar 3000). The samples were pretreated at 300 °C for 3 h in vacuum.

Powder X-ray diffraction (XRD) characterization was carried out on a X′ Pert Pro automatic powder diffractometer operated at 40 kV and 30 mA, using Cu Kα (λ = 0.15406 nm) monochromatized radiation in all cases. Each step of 0.0167° was measured for 10 s from 10° to 90° (2θ). JCPDS file database was used for peak identification.

Raman spectra were recorded with a Renishaw-UV-Vis Raman System 1000 equipped with a CCD detector at room temperature. The 325 nm of the He–Cd laser was used as the exciting source with a power of 30 mW.

Acid properties which were determined by ammonia temperature-programmed desorption (NH_3-TPD) were measured in a Micromeritics AutoChem II 2920 analyzer. 0.2 g of catalyst sample was filled in a U-shaped quartz reactor tube and a thermocouple was placed onto the top of sample. All samples were pretreated in He (20 ml min^{-1}) at 400 °C for 2 h then in H_2 (20 ml min^{-1}) for 1 h. After cooling down to 100 °C, 5%NH_3/He was passed over the samples for 30 min. Then, the samples were swept with helium for 60 min and finally the desorption step was performed from 100 °C to 700 °C at a heating rate of 10 °C min^{-1} and with a helium flow of 30 ml min^{-1}. The desorbed products were monitored by a TCD and a MS equipment simultaneously.

Temperature-programmed desorption of hydrogen (H_2-TPD) measurements were done in a Micromeritics AutoChem II 2920 analyzer. 0.2 g of catalyst sample was filled in a U-shaped quartz reactor tube and a thermocouple was placed onto the top of sample. All samples were pretreated in He (20 ml min^{-1}) at 400 °C for 2 h then in H_2 (20 ml min^{-1}) for 1 h. After cooling down to 50 °C, the samples were swept with helium for 60 min and finally the desorption step was performed from 50 °C to 700 °C at a heating rate of 10 °C min^{-1} and 30 ml min^{-1} of helium total flow.

X-ray photoelectron spectra were collected using a VG MiltiLab 2000 spectrometer with Mg Kα radiation and a multichannel detector. Binding energies (BE) corresponding to Ni 2p electrons were referenced to C 1s line, taken as 284.6 eV.

FT-IR spectra were used to characterize the structure of catalysts before and after the reaction. IR spectra of the catalysts were recorded using a Thermo Nicolet Nexus spectrometer equipped with a liquid-nitrogen-cooled MCT detector.

FT-IR spectra of pyridine adsorption were recorded using a Thermo Nicolet Nexus spectrometer equipped with a liquid-nitrogen-cooled MCT detector. The samples were pressed into self-supporting wafers and treated in H_2 at 300 °C in an IR cell for 1 h followed by evacuation at 300 °C for 5 min to remove the gas phase H_2. After cooling to 100 °C, the samples were exposed to pyridine vapor for 10 min. Then the spectra were recorded after evacuation at high temperatures. The IR spectra were recorded in the spectral range 1700–1400 cm^{-1} with 32 scans and at a resolution of 4 cm^{-1}.

2.3. Catalysts performances for hydrocracking activities

Decane used in the present study was commercially available reagent without further purification. The catalytic performance of the catalysts was measured in a down flow fixed-bed quartz tube reactor cased in a stainless steel tube (8 mm id; 150 cm in length) at 2.0 MPa, LHSV 4 h^{-1} and H_2/*n*-decane volume ratio of 1500. The products were collected and identified when the reaction had begun for 4 h. The products were separated by condensation, the gas products were analyzed by gas chromatograph with a Porapak Q column (3 m) and TCD detector and the liquid products were analyzed by an OV-101 capillary column (30 m) and FID detector.

Prior to reaction, all the catalysts were reduced by a flow of H_2 at 300 °C for 1 h or sulfided at 300 °C for 8 h using a flow of CS_2/H_2 (60 $cm^3\ min^{-1}$, volume ratio 5/95). To know whether

the reduced catalysts can resist poisoning by organic sulfur and nitrogen compounds, the *n*-decane with 750 ppm thiophene and 500 ppm pyridine was also used as the feedstock and the experimental conditions were the same as that of the hydrocracking of *n*-decane mentioned above.

For comparison, a commercial hydrocracking catalyst disclosed in Chinese patent CN1393521 was also measured for hydrocracking of *n*-decane under the same conditions.

3. Results and discussion

3.1. Dispersion of $H_3PW_{12}O_{40}$ on the catalysts

Table 1 shows the specific surface areas measured by the BET method, and the composition of the catalysts without calcination. It can be seen from Table 1 that the surface area of the catalysts decreases with the increase of $H_3PW_{12}O_{40}$ content. The decrease of the surface area is found to be even more pronounced for 5%Ni-60%$H_3PW_{12}O_{40}$/SiO_2 samples, perhaps being due to pore blockage.

The XRD patterns of Ni-$H_3PW_{12}O_{40}$/SiO_2 catalysts without calcination are shown in Fig. 1. It is clear that no diffraction peak of NiO appeared for the catalysts with the fixed amount of 5% Ni. Although, the intensities are changed due to the influence of silica, the characteristic diffraction peaks of $H_3PW_{12}O_{40}$ phase are still observed and their intensity increase with the increasing of the amount of $H_3PW_{12}O_{40}$ on the catalysts. Furthermore, we found that the characteristic diffraction peaks have a little change when the $H_3PW_{12}O_{40}$ doped onto the silica which had been presented by some papers [11–13].

The Raman spectra of the catalysts are shown in Fig. 2. All the Ni-$H_3PW_{12}O_{40}$/SiO_2 samples without calcination display similar Raman spectra. The sharp and intense bands at 1012 cm^{-1} most likely correspond to stretching vibrations of P–O bond of $P–O_4$, whereas bands at lower wave-numbers are attributed to $W{=}O_d$ (988 cm^{-1}) and $W–O_b–W$ (930 cm^{-1}) vibrations [14]. Its intensity increases with the increase of the amount of the $H_3PW_{12}O_{40}$ in the catalysts. Although changes occurred in the spectra compared to the pure $H_3PW_{12}O_{40}$, no degradation products or bulk WO_3 were identified.

In summary, when the $H_3PW_{12}O_{40}$ contents of the catalysts are less than 40%, $H_3PW_{12}O_{40}$ will be highly dispersed on the support.

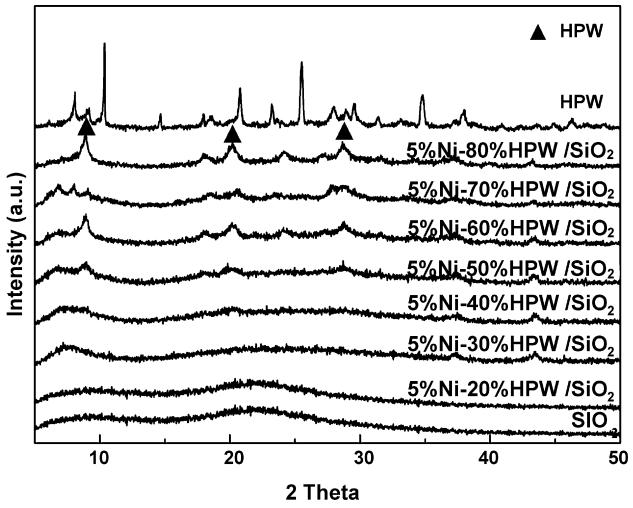

Fig. 1. XRD patterns of Ni-$H_3PW_{12}O_{40}$/SiO_2 catalysts with the different contents of $H_3PW_{12}O_{40}$.

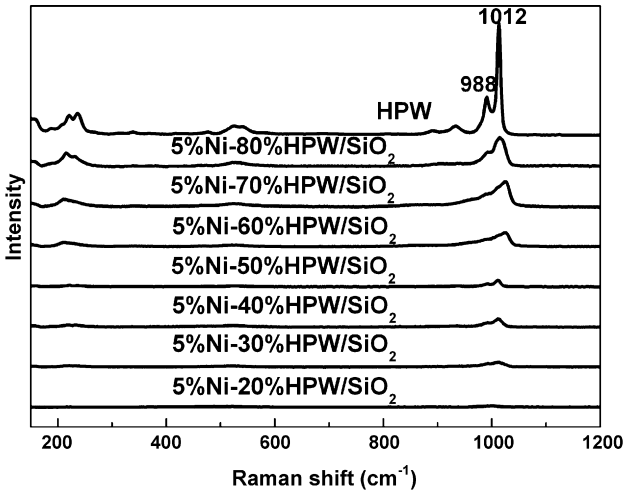

Fig. 2. Raman patterns of Ni-$H_3PW_{12}O_{40}$/SiO_2 catalysts with the different contents of $H_3PW_{12}O_{40}$.

3.2. Stability of $H_3PW_{12}O_{40}$

In some papers, $H_3PW_{12}O_{40}$ seemed to be easily decomposed. Thus, we also studied characters of the catalysts calcined at different temperatures so as to understand the stability of

Table 1
Composition and physical properties of the oxidized catalysts*

Catalysts	Surface area (m^2 g^{-1})	Pore size (nm)	Ni (wt%)	$H_3PW_{12}O_{40}$ (wt%)
SiO_2	406	9.6	0	0
5%Ni/SiO_2	361	9.5	5	0
50%$H_3PW_{12}O_{40}$/SiO_2	211	7.9	0	50
10%Ni-50%$H_3PW_{12}O_{40}$/SiO_2	166	7.2	10	50
15%Ni-50%$H_3PW_{12}O_{40}$/SiO_2	142	6.4	15	50
5%Ni-30%$H_3PW_{12}O_{40}$/SiO_2	255	8.6	5	30
5%Ni-40%$H_3PW_{12}O_{40}$/SiO_2	220	8.1	5	40
5%Ni-50%$H_3PW_{12}O_{40}$/SiO_2	200	7.6	5	50
5%Ni-60%$H_3PW_{12}O_{40}$/SiO_2	144	6.3	5	60
Commercial catalyst	275	4.9		

* These catalysts are not calcined.

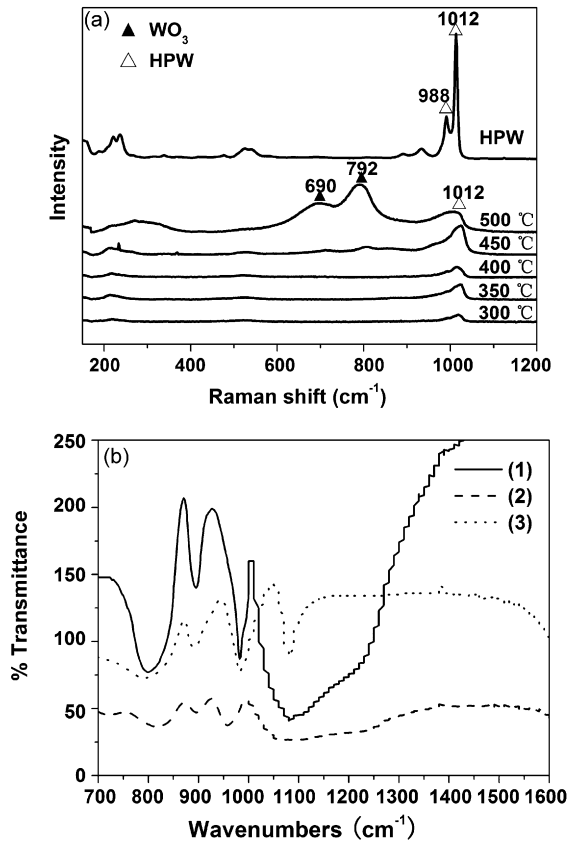

Fig. 3. (a) Raman spectra of 5%Ni-50%$H_3PW_{12}O_{40}$/SiO_2 catalysts calcined at different temperature. (b) IR spectra (1) 5%Ni-50%$H_3PW_{12}O_{40}$/SiO_2 catalysts before reaction, (2) 5%Ni-50% $H_3PW_{12}O_{40}$/SiO_2 catalysts after reaction and (3) $H_3PW_{12}O_{40}$.

$H_3PW_{12}O_{40}$ in the Ni-$H_3PW_{12}O_{40}$/SiO_2 catalysts after heating treatment. The Raman spectra of samples 5%Ni-50%$H_3PW_{12}O_{40}$/SiO_2 calcined at different temperatures are shown in Fig. 3a. When the calcining temperature is lower than 450 °C, the Raman spectra of the catalysts only showed the bands assigned to $H_3PW_{12}O_{40}$. In the spectra of catalyst calcined at 450 °C, some changes occurred, especially in the range 900–700 cm^{-1}. This region is related to the stretching vibrations of the bridges between tritungstate groups of the Keggin structure, sensitive to the dehydration process induced by the thermal treatment [15,16]. Two new bands at 792 cm^{-1} and 690 cm^{-1} attributed to W–O–W and W=O stretching modes were observed and could be assigned to crystalline WO_3 [17]. In the higher temperature (500 °C), the WO_3 bands dominated the spectra. These results indicate that $H_3PW_{12}O_{40}$ decomposes when the calcining temperature exceeds 450 °C.

In addition, it is more important to look into the change of $H_3PW_{12}O_{40}$ during the reaction, and therefore FT-IR was used to characterize the structure of catalysts before and after the reaction. IR spectra of the catalysts are presented in Fig. 3b. It is well known that Keggin type $PW_{12}O_{40}^{3-}$ ions exhibit characteristic absorption bands of: υP–O (1080 cm^{-1}), υW=O O (980 cm^{-1}) and υW–O–W (890 cm^{-1} and 795 cm^{-1}). These bands were observed for the samples before and after the reaction. Furthermore, the band due to W=O in the catalyst after the reaction was found to shift toward the direction of lower wave-number, indicating that the structure of the Keggin type $PW_{12}O_{40}^{3-}$ ions in the catalysts has not been destroyed, while the W=O bond has been weakened. It seems to us that this observation is probably due to chemical interaction between $H_3PW_{12}O_{40}$ and metal Ni.

3.3. Acidic property of the catalysts

To examine the acidic property of the Ni-$H_3PW_{12}O_{40}$/SiO_2 catalysts, NH_3-TPD was carried out and the spectra are shown in Fig. 4a and two desorption peaks of ammonia at 200 °C and 450 °C, respectively can be detected. As the amount of $H_3PW_{12}O_{40}$ increases, the amount of NH_3 desorbed increases. The acid strength of these samples is consistent with the activity of the catalysts (shown in Fig. 5a) except that the activity of 5%Ni-60%$H_3PW_{12}O_{40}$/SiO_2 catalysts is lower than that of 5%Ni-50%$H_3PW_{12}O_{40}$/SiO_2 catalysts, which might be due to

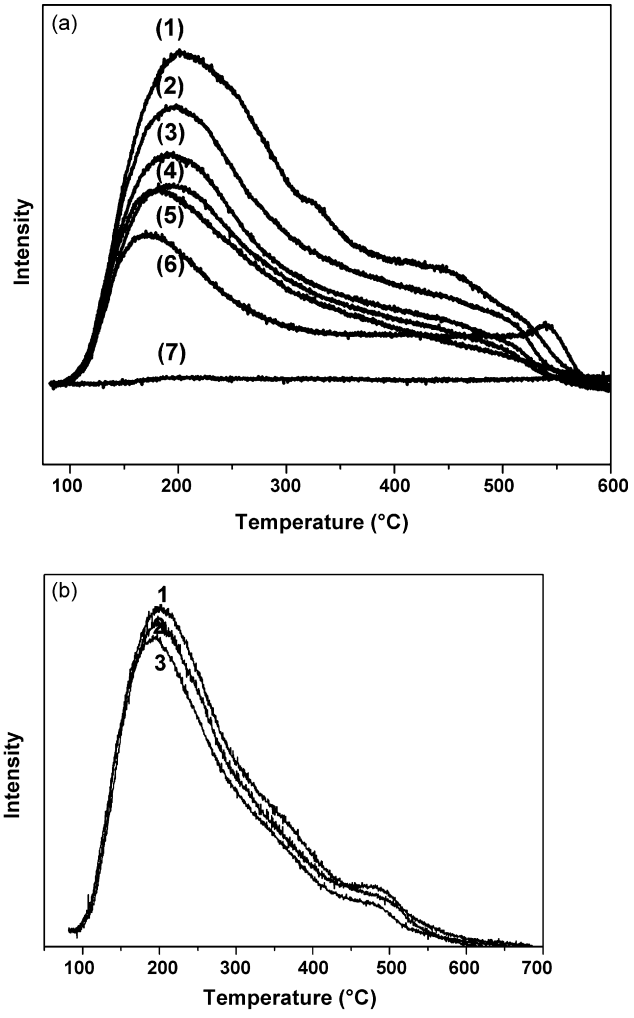

Fig. 4. (a) NH_3-TPD profiles of reduced catalysts (1) 5%Ni-60%$H_3PW_{12}O_{40}$/SiO_2, (2) 5%Ni-50%$H_3PW_{12}O_{40}$/SiO_2, (3) 5%Ni-40%$H_3PW_{12}O_{40}$/SiO_2, (4) 5%Ni-30%$H_3PW_{12}O_{40}$/SiO_2, (5) commercial catalyst, (6) 50%$H_3PW_{12}O_{40}$/SiO_2 and (7) 5%Ni/SiO_2. (b) NH_3-TPD profiles of reduced catalysts (1) 5%Ni-50%$H_3PW_{12}O_{40}$/SiO_2, (2) 10%Ni-50%$H_3PW_{12}O_{40}$/SiO_2 and (3) 15%Ni-50%$H_3PW_{12}O_{40}$/SiO_2.

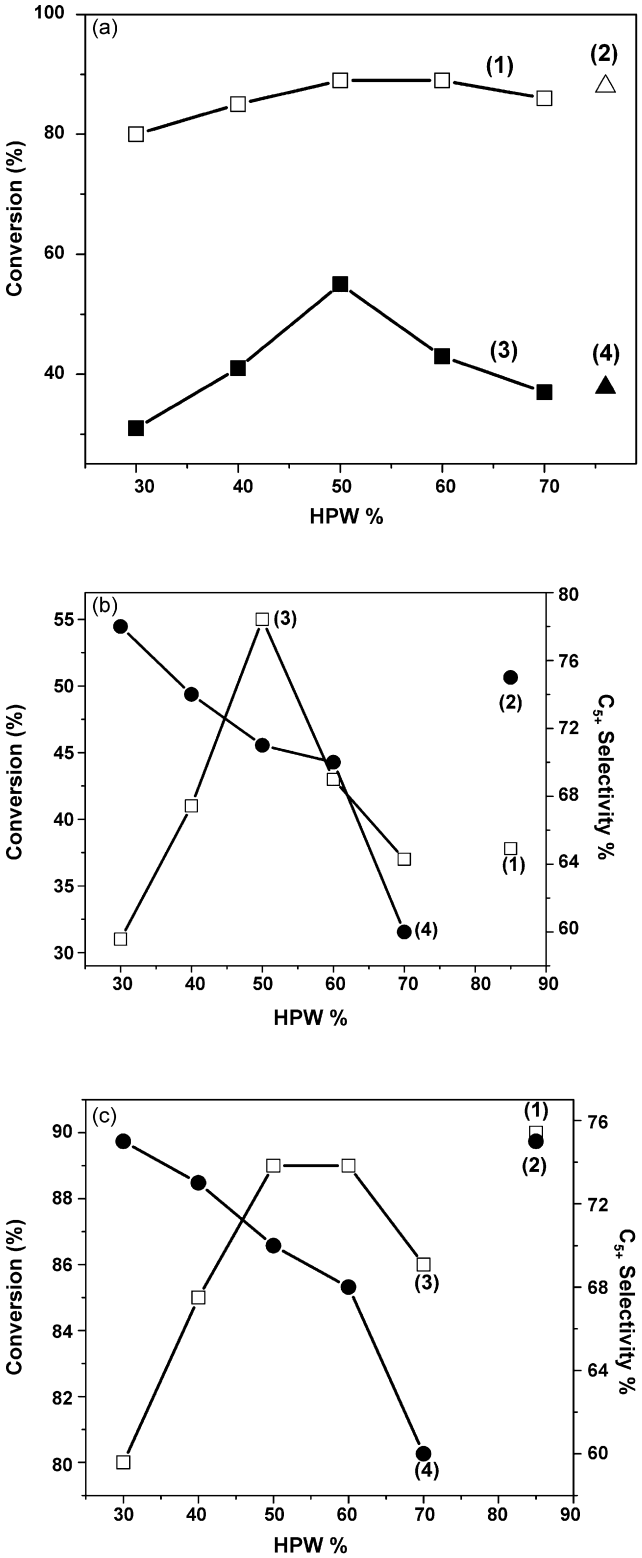

Fig. 5. (a) Comparison of different catalysts for hydrocracking of *n*-decane (1) reduced 5%Ni-$H_3PW_{12}O_{40}/SiO_2$, (2) reduced commercial catalyst, (3) sulfided 5%Ni-$H_3PW_{12}O_{40}/SiO_2$ and (4) sulfided commercial catalyst. Reaction conditions: $T = 300$ °C; H_2/decane = 1500; $P = 2$ Mpa and LHSV = 2 h^{-1}. (b) Comparison of different catalysts for hydrocracking of *n*-decane (1) conversion over sulfided commercial catalyst, (2) C_5^+ selectivity over sulfided commercial catalyst, (3) conversion over sulfided 5%Ni-$H_3PW_{12}O_{40}/SiO_2$ and (4) C_5^+ selectivity over sulfided 5%Ni-$H_3PW_{12}O_{40}/SiO_2$. Reaction conditions: $T = 300$ °C; H_2/decane = 1500; $P = 2$ Mpa and LHSV = 2 h^{-1}. (c) Comparison of different catalysts for hydrocracking of *n*-decane (1) conversion over reduced commercial catalyst, (2) C_5^+ selectivity over reduced commercial catalyst, (3) conversion over reduced 5%Ni-$H_3PW_{12}O_{40}/SiO_2$ and (4) C_5^+ selectivity over reduced 5%Ni-$H_3PW_{12}O_{40}/SiO_2$. Reaction conditions: $T = 300$ °C; H_2/decane = 1500; $P = 2$ Mpa and LHSV = 2 h^{-1}.

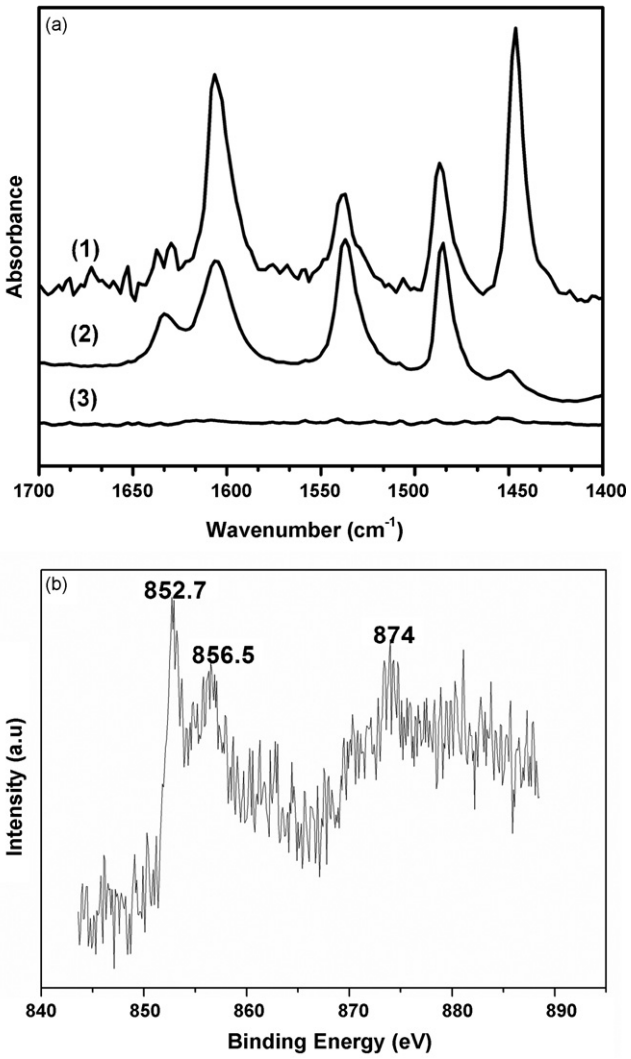

Fig. 6. (a) FT-IR spectra of pyridine absorbed on reduced catalysts (1) 5%Ni-50%$H_3PW_{12}O_{40}/SiO_2$, (2) 50%$H_3PW_{12}O_{40}/SiO_2$ and (3) 5%Ni/SiO_2. (b) Ni 2p photoelectron spectra of reduced 10%Ni-50% $H_3PW_{12}O_{40}/SiO_2$ catalysts.

the decrease of the surface areas with the increasing content of $H_3PW_{12}O_{40}$ in the catalysts or the unsuitable metal/acid ratio. It seems that the acidity of the catalyst may not simply account for the catalytic activity. The NH_3-TPD experiment, which is taken to display the function of interrelation of the metal and acid sites on the catalysts, shows a great increase of the total acid number of the catalysts after loading of Ni upon the $H_3PW_{12}O_{40}/SiO_2$ catalysts. The result indicates that the change of acid sites of the catalysts can be attributed to the promotion of metal Ni or some interaction between these two sites happened.

Furthermore, to know the acidity of the catalysts with more Ni contents, the NH_3-TPD measurements of the catalysts 5%Ni-50%$H_3PW_{12}O_{40}/SiO_2$, 10%Ni-50%$H_3PW_{12}O_{40}/SiO_2$,

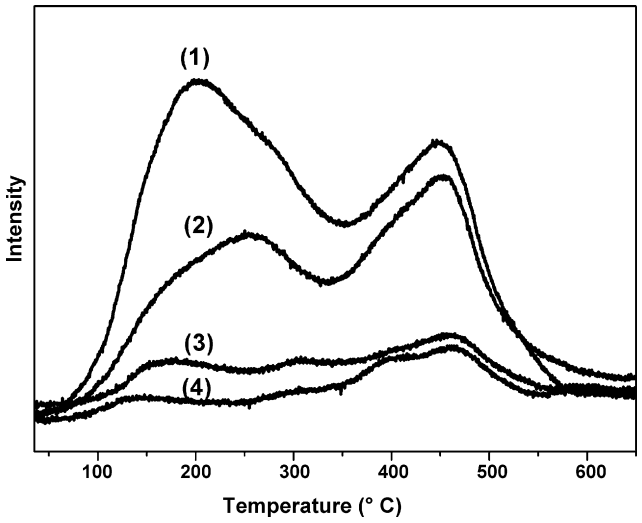

Fig. 7. H_2-TPD profiles of catalysts (1) 5%Ni-60%$H_3PW_{12}O_{40}/SiO_2$, (2) 5%Ni-50%$H_3PW_{12}O_{40}/SiO_2$, (3) 5%Ni-40%$H_3PW_{12}O_{40}/SiO_2$ and (4) 5%Ni-30%$H_3PW_{12}O_{40}/SiO_2$.

15%Ni-50%$H_3PW_{12}O_{40}/SiO_2$ were carried out and the spectra are shown in Fig. 4b. It is clear from Fig. 4b that as the amount of Ni increases, the amount of NH_3 desorbed decreases and consequently the acidity of the catalysts decreases, indicating that the much more Ni promotion will decrease the acidity of the catalysts.

FT-IR was also used to characterize the nature of acid sites by pyridine desorption on very thin self-supporting wafers of Ni-$H_3PW_{12}O_{40}/SiO_2$ catalysts. The spectra of pyridine desorbed at 300 °C are shown in Fig. 6a. The bands around 1450 cm^{-1} and 1610 cm^{-1} are typical of pyridine adsorbed at Lewis acid centers while the bands around 1542 cm^{-1} are evidence for the formation of pyridinium cations resulting from adsorption at Brönsted acid sites [18,19]. The band around 1490 cm^{-1} contains contributions from both forms of adsorbed pyridine. The results show that the acidity of 5%Ni/SiO_2 catalyst is so low that the absorption bands for acid sites almost cannot be detected in the IR spectra. The IR spectra of 5%Ni-50%$H_3PW_{12}O_{40}/SiO_2$ show more intense absorption bands for Lewis acidity (1445 cm^{-1}) comparing to that of the 50% $H_3PW_{12}O_{40}/SiO_2$ sample.

It demonstrates that there are some new Lewis acid sites appearing in the Ni-$H_3PW_{12}O_{40}/SiO_2$ catalysts after the loading of the nickel, which would probably be due to the existence of electron-deficient metal sites which exhibit great Lewis acidity as a result of the interaction between the metal sites and the acid sites.

To investigate the state of Ni in the Ni-$H_3PW_{12}O_{40}/SiO_2$ catalysts, a XPS test for the reduced catalysts 10%Ni-50%$H_3PW_{12}O_{40}/SiO_2$ was made (shown in Fig. 6b). The three main peaks in the Ni 2p spectra were assigned to the spin-splitting Ni $2p_{3/2}$ (BE 852.7 eV, 856.5 eV) and Ni $2p_{1/2}$ (BE 874 eV). The intense peaks of Ni $2p_{3/2}$ appear at 852.7 eV which showed the presence of Ni^0 after reduction. The Ni $2p_{3/2}$ peak at about 856.5 eV was also due to the presence of non-reduced Ni^{2+} species. The result indicates that the nickel species on the reduced catalyst are not only in the zero valent state but also present as Ni^{2+} species.

3.4. H_2-absorbed behaviour on the catalysts

The metal properties of reduced Ni-$H_3PW_{12}O_{40}/SiO_2$ catalysts were studied by H_2-TPD (Fig. 7). The H_2-TPD profiles show that all the Ni-$H_3PW_{12}O_{40}/SiO_2$ catalysts exhibit two H_2 desorbed peaks at 260 °C and 470 °C, respectively. The amount of H_2 desorbed in the low temperature stage increases with the increasing of the amount of $H_3PW_{12}O_{40}$ in the catalysts.

According to the classical bifunctional metal–acid mechanism, the metal sites were involved in the initial alkane activation through dehydrogenation, while others suggested the *n*-alkane reactant took place in a redox step involving the other promotion of support [20]. These models successfully explained a number of experimental observations, but failed to account for the role of hydrogen and the synergy between the two catalyst components [21]. Thus the hydrogen spillover is now a well-known phenomenon in heterogeneous catalysis. A number of excellent reviews on the subject have been published.

In our study, the increase of the amount of $H_3PW_{12}O_{40}$ with the same amount of the nickel content of the catalysts can be explained by a non-classical bifunctional mechanism. On one hand, the role of $H_3PW_{12}O_{40}$ is not only as an acid site but also a hydro-dehydrogenation site in which the hydrocracking can take place in a redox step just as the non-classic mechanism reported in some papers [20]. On the other hand, taking into account of the results of the H_2-TPD experiment, the conclusion that the desorption trend of H_2 on the catalysts are mostly ascribed to the hydrogen spillover can be drown [21], which has been used as an important mechanism in hydrogeneous catalysis. It suggests that the metal Ni dissociates molecule hydrogen to highly reactive hydrogen species (i.e. H^+, H^-, $H^{\delta+}$) or ion pair [22,23] which will easily result in the

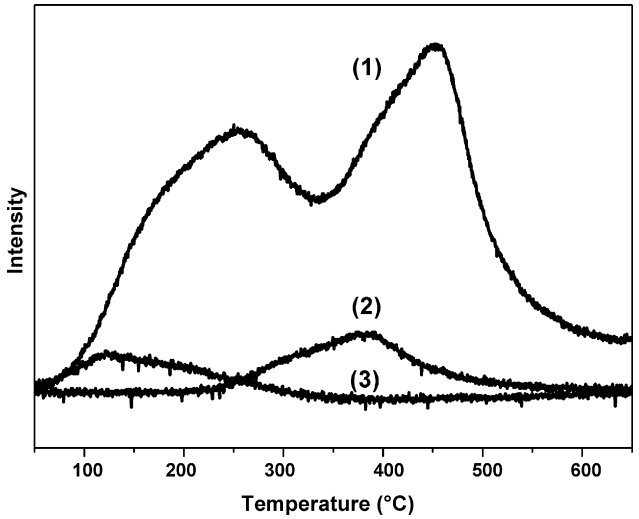

Fig. 8. H_2-TPD profiles of catalysts (1) 5%Ni-50%$H_3PW_{12}O_{40}/SiO_2$, (2) 5%Ni/SiO_2 and (3) 50%$H_3PW_{12}O_{40}/SiO_2$.

formation of products on the catalyst by dehydrogenation which can react with the proton on the Brönsted site to form a carbonium ion, and then the carbonium ion combine with the migrate hydride ion from a Lewis site to produce a saturated compounds [20,22–24]. Further study using three catalysts: 5%Ni-50%$H_3PW_{12}O_{40}/SiO_2$, 5%Ni/SiO_2 and 50%$H_3PW_{12}O_{40}/SiO_2$ indicates that the 5%Ni/SiO_2 catalyst only has one H_2-absorbed stage at lower temperature region and the 50%$H_3PW_{12}O_{40}/SiO_2$ catalyst has one H_2-absorbed stage at higher temperature (shown in Fig. 8). The two H_2-desorbed stages which possessing of much more amount of the H_2 desorbed than those two catalysts mentioned above displayed on the 5%Ni-50%$H_3PW_{12}O_{40}/SiO_2$ catalysts, also accord with the hydrogen spillover mechanism.

3.5. Activity and selectivity of n-decane hydrocracking

The evaluation results of the reduced and sulfided Ni-$H_3PW_{12}O_{40}/SiO_2$ catalysts with different Ni/$H_3PW_{12}O_{40}$ weight ratio for hydrocracking of *n*-decane were shown in Fig. 5a–c, wherein the conversion of *n*-decane and the yield of C_5^+ were taken to express the activity of the catalyst and the selectivity of desired liquid products, respectively. To compare the catalytic performance of the catalysts with typical industrial catalysts, a commercial catalyst containing zeolite were also evaluated. It can be seen from Fig. 5a that for both the reduced and sulfided 5%Ni-$H_3PW_{12}O_{40}/SiO_2$ catalysts, when $H_3PW_{12}O_{40}$ content in the catalyst equal to 50%, the conversions of *n*-decane all reached maximum, but the activity of reduced catalysts is found to be higher than that of sulfided catalysts.

The results also show that reduced Ni-$H_3PW_{12}O_{40}/SiO_2$ catalysts exhibit just the same activity as that of the reduced commercial catalyst for the hydrocracking of *n*-decane, while the sulfided Ni-$H_3PW_{12}O_{40}/SiO_2$ catalysts show higher activity than sulfided commercial catalyst. The observation that the activity of the sulfided Ni-$H_3PW_{12}O_{40}/SiO_2$ catalysts can be enhanced by increasing the content of $H_3PW_{12}O_{40}$ in catalysts until the content of $H_3PW_{12}O_{40}$ exceeds 50% could be explained by the balance between the metal and acid site along with the increasing $H_3PW_{12}O_{40}$ content. In addition, it can be seen from Fig. 5b and c that the higher the contents of $H_3PW_{12}O_{40}$ of the catalysts, the lower the C_5^+ selectivity over the catalysts.

3.6. Sulfur and nitrogen-tolerance

Although, large quantity of organic sulfur and nitrogen compounds had been removed during the pretreatment of the feedstock, small amounts of sulfur and nitrogen compounds are still present in the feedstock, so the resistance of catalysts to sulfur and nitrogen compounds was required indeed.

In order to know whether the reduced catalyst can resist the poisoning by organic sulfur and nitrogen compounds, given quantity of thiophene and pyridine were incorporated into *n*-decane to produce a mixed feedstock with 750 ppm thiophene and 500 ppm pyridine. The experiment results are shown in Fig. 9. It is clear that both of the activities of the reduced Ni-$H_3PW_{12}O_{40}/SiO_2$ catalysts and the reduced commercial catalyst are significantly suppressed, while the activity of the reduced Ni-$H_3PW_{12}O_{40}/SiO_2$ catalysts is much higher than that of the reduced commercial catalyst. In Fig. 9, the C_5^+ selectivity over reduced Ni-$H_3PW_{12}O_{40}/SiO_2$ catalysts with different Ni/$H_3PW_{12}O_{40}$ weight ratio as well as a commercial catalyst is compared.

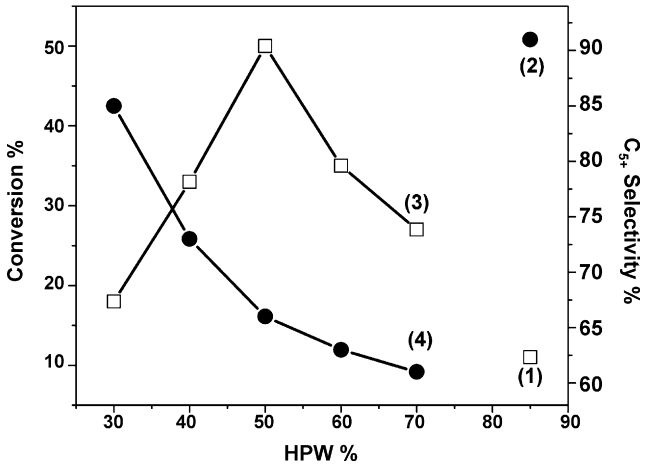

Fig. 9. Comparison of reduced catalysts for hydrocracking of *n*-decane with 750 ppm thiophene and 500 ppm pyridine (1) conversion over reduced commercial catalyst, (2) C_5^+ selectivity over reduced commercial catalyst, (3) conversion over reduced 5%Ni-$H_3PW_{12}O_{40}/SiO_2$ and (4) C_5^+ selectivity over reduced 5%Ni-$H_3PW_{12}O_{40}/SiO_2$. Reaction conditions: $T = 300\ ^\circ C$; H_2/decane = 1500; $P = 2$ Mpa and LHSV = 2 h^{-1}.

Many papers proposed that sulfur makes the active metal sites poisoned, resulting in loss of hydrogenation activity; while nitrogen makes the acidic sites poisoned, resulting in a low activity [6,7]. Sulfur tolerance has been shown to be related to the formation of electron-deficient metal sites, which in turn weaken the strength of the sulfur–metal bond [25]. It seems to us that the electron-deficient sites can be formed because of the intense Brönsted acid site of the $H_3PW_{12}O_{40}$. Moreover, because of the hydrogen spillover, the catalyst with a reactive hydrogen layer covering with the surface, which can promote the formation of the metal-S, thus, represent a better resistance to the sulfur compounds.

4. Conclusion

The results obtained in the present work indicate that the Ni-$H_3PW_{12}O_{40}/SiO_2$ catalysts show high activity for *n*-decane hydrocracking. For both the reduced and sulfided 5%Ni-$H_3PW_{12}O_{40}/SiO_2$ catalysts, when $H_3PW_{12}O_{40}$ contents in the catalyst equal to 50%, the conversions of *n*-decane all reached maximum, but the activity of reduced catalyst is found to be higher than that of sulfided catalyst even in the presence of nitrogen and sulfur-containing compounds in the feedstock. The high activity of Ni-$H_3PW_{12}O_{40}/SiO_2$ catalysts for the *n*-decane hydrocracking may be due to the unique structure of the $H_3PW_{12}O_{40}$ which is a bifunctional material having both great acidity and the hydro-dehydrogenation function and the interaction between metal Ni and $H_3PW_{12}O_{40}$ which offers the sufficient reactive hydrogen partially by the hydrogen

spillover on the surface of the catalysts that had been discussed above.

Acknowledgement

This project is supported by the Ministry of Science and Technology of China (2004CB217805).

References

[1] M. Roussel, J.L. Lemberton, J. Catal. 218 (2003) 427.
[2] A. Corma, Catal. Lett. 22 (1993) 33.
[3] A. Hennico, A. Billon, P.H. Bigeard, J.P. Peries, Rev. Inst. Français. Pétrol. 48 (1993) 127.
[4] J.K. Minderhoud, J.A.R. Van. Veen, A.P. Hagan, Stud. Surf. Sci. Catal. 127 (1999) 3.
[5] C. Marcilly, J. Catal. 217 (2003) 47.
[6] D. Eliche-Quesada, J.M. Merida-Robles, E. Rodriguez-Castellon, A. Jimenez-Lopez, Appl. Catal. A 65 (2006) 118.
[7] M. Roussel, S. Norsic, Appl. Catal. A 279 (2005) 53.
[8] K. Ahmed, Appl. Catal. A 303 (2006) 141.
[9] M. Misono, Chem. Commun. (2001) 1141.
[10] H. Firouzabadi, N. Iranpoor, K. Amani, Green Chem. 3 (2001) 131.
[11] Q. Wu, S. Tao, G. Meng, Mater. Sci. Eng. B 68 (2000) 161.
[12] G.S. Kumar, M. Vishnuvarthan, V. Murugesan, J. Mol. Catal. A 260 (2006) 49.
[13] J.C. Yori, Appl. Catal. A 286 (2005) 71.
[14] X. Qu, Y. Guo, C. Hu, J. Mol. Catal. A 262 (2007) 128.
[15] C.R. Deltcheff, M. Fournier, R. Franck, Inorg. Chem. 22 (1983) 207.
[16] S. Damyanova, J.L.G. Fierro, Chem. Mater. 10 (1998) 871.
[17] J.R. Sohn, M.Y. Park, Langmuir 14 (1998) 6140.
[18] K. Sato, Y. Iwata, Catal. Today 45 (1998) 367.
[19] C. Breen, A.T. Deane, J.J. Flynn, Clay Miner. 22 (1987) 169.
[20] S. Kuba, P. Lukinskas, R.K. Grasselli, B.C. Gates, H. Knozinger, J. Catal. 216 (2003) 353.
[21] A. Martinez, G. Prieto, Appl. Catal. A 309 (2006) 224.
[22] M.M. Hossain, J. Chem. Eng. 123 (2006) 15.
[23] V.M. Benitez, J.C. Yori, Energy Fuel 20 (2006) 422.
[24] H. Du, C. Fairbridge, Appl. Catal. A 294 (2005) 1.
[25] C.A. Emeis, J. Catal. 141 (1993) 347.